

Wind and Ice Load Model Using Numerical Weather Prediction

Petr Musilek, Pawel Pytlak
Electrical & Computer Engineering
University of Alberta
Edmonton, AB, Canada
E-mail: musilek@ece.ualberta.ca

Edward Lozowski
Earth & Atmospheric Sciences
University of Alberta
Edmonton, AB, Canada

Dan Arnold
Alberta Environment
Edmonton, AB, Canada

Janos Toth
British Columbia Transmission Corporation
Vancouver, BC, Canada

Abstract—This paper describes a forecasting model that can be used by utilities to estimate wind and ice storm impact on electric power grids. The grids are exposed to weather conditions that can cause damage resulting in temporary loss of service. Because the reliability of power transmission networks is of crucial importance to society, the ability to predict potential hazards and to plan possible mitigation measures in advance is of great interest. In this study, we concentrate on prediction of combined ice and wind loads, which cause most failures of overhead conductors and other components of power networks. Modeling of these loads requires estimation of forces exerted on the conductors due to wind and ice build up. The proposed system approaches this modeling problem in four stages. First, meteorological conditions in the area of interest are determined using a Numerical Weather Prediction (NWP) model. Second, NWP output is processed to obtain factors pertinent for wind and ice modeling: occurrence of freezing precipitation, precipitation rate, temperature, and wind velocity. These variables are derived from NWP model output and corrected for the height of overhead conductors. The third stage involves an ice accretion model, which is engaged depending on the temperature and precipitation type. Fourth, a force model then calculates the force due to the weight of the ice, and the force of wind acting on the ice covered conductor. The resulting forces are then combined to determine the total load on the conductor. The system has been developed and verified using field data provided by the British Columbia Transmission Corporation (BCTC), Canada. The results indicate a good match between timing of peak forces determined by the system and observed outages. BCTC plans to explore the implementation of this forecasting system as a tool to support the operation of their transmission system.

I. INTRODUCTION

Weather events play a major role in the operability of electric power systems. Meteorological conditions impact not only power production and consumption patterns, but also the integrity of the power transmission infrastructure and characteristics of the transmission network [1]. Weather phenomena that can cause transmission line failures include: severe wind, extreme ice loads, combined wind and ice loads, lightning strikes, conductor vibrations and galloping, avalanches, landslides, and flooding [2], [3]. Excessive icing on overhead transmission lines can cause outages resulting in repair costs

of millions of dollars [4]. Thus, the objective of the work presented in this paper is to forecast the additional force load on power line conductors caused by ice accretion during periods of freezing rain, by combining a state-of-the-art NWP system with a precipitation type determination algorithm, freezing rain ice accretion model, and a conductor loading model.

II. BACKGROUND

In a study conducted by the International Council on Large Electric Systems (CIGRE), transmission system failures that occurred worldwide between 1991 and 1996 were examined. Wind, ice, and combined wind and ice loads were the three top causes of damage, resulting in 87% of the total damage suffered by transmission lines [3]. Accreted ice can damage transmission systems in several ways: excess weight on the conductors may break them; excess weight on nearby tree limbs may cause them to fall onto conductors, and ice accretions create larger exposed surface areas resulting in greater wind loads and the possibility of galloping.

Although icing events are rare, they are very costly. For example, an ice storm in mid January of 1998 brought prolonged icing events to many parts of Quebec, Ontario, and the north-eastern U.S., resulting in a radial equivalent freezing rain accumulations of up to 70 mm. This single storm caused an estimated 1.44 billion dollars insured loss, the greatest in the history of Canada [5]. It interrupted electrical power for 5.2 million people in Canada and the U.S. and resulted in 25 fatalities. An early warning system would have allowed the population to be better prepared for this disaster. Additionally, a system built to predict potential transmission system damage would have allowed transmission companies to take preventive measures before the storm hit.

Current detection methods include costly visual inspection either by helicopter, airplane, or motor vehicle; or analysis of readings obtained from tower sensors. Unfortunately, on tower sensors are prone to failure since they are exposed to the same meteorological conditions as the power lines. Also,

because the cost of obtaining, installing and maintenance of on tower sensors, they are only installed in select locations of a transmission network. In contrast, computer modeling systems can be run from a centralized location, and at a relatively low cost. They can be used to hindcast ice accumulations during historical events, allowing researchers to assess long term trends, or they can be used to forecast future events. Additionally, computer models offer complete coverage for the transmission network. For these reasons, modeling and forecasting ice accretion on transmission networks represents a significant economic opportunity for the power transmission and distribution industry. Several studies have used computer models to predict freezing rain events; however, the development of models using state-of-the-art numerical weather prediction (NWP) systems has not yet been fully explored.

III. WIND AND ICE LOAD MODEL

The Wind and Ice Load Model (WILM) presented in this paper is comprised of four main components: a numerical weather prediction model, a precipitation type diagnostic model, an ice accretion model, and a wind and ice load force model. A NWP model is used to forecast/hindcast meteorological conditions over an area of interest. The meteorological variables are then used by the precipitation type model to determine whether freezing rain is occurring. If freezing rain is diagnosed, the icing model is called to model the equivalent radial ice accreted on a transmission or distribution system conductor. It is important to note that the WILM system actually implements the icing model based on a fuzzy implementation of an engagement factor. Finally, WILM calculates the excess force on the conductor by considering the ice mass and the wind acting on the ice-coated conductor.

A. Numerical Weather Prediction

To provide effective ice accretion forecasts, an accurate and efficient Numerical Weather Prediction (NWP) system must be used. It must be available at low cost and have user support; produce reliable and accurate forecasts; have the ability to hindcast meteorological conditions; and be capable of being run on a highly parallelized architecture in order to produce simulations within a reasonable time frame.

To meet the aforementioned criteria, the Advanced Weather Research and Forecasting (WRF) NWP system was chosen. It contains cutting edge and configurable modules, is capable of providing high-resolution mesoscale forecasts, and has recently been adopted by the National Centers for Environmental Prediction as the operational forecast model for the United States. The WRF model is designed to be a flexible, state-of-the-art forecast system written using portable code that is efficient in a massively parallel computing environment [6].

The selected ARW core is based on an Eulerian solver for the fully compressible, non-hydrostatic primitive equations. The state variables are solved in scalar-conserving flux form on a mass-based, terrain-following vertical coordinate grid. The ARW core is controlled by numerous user-selected physics and

dynamics schemes allowing the WRF model to be optimized for different applications.

Because WRF is run as a regional NWP model, it must be initialized with boundary conditions from either a global weather model and/or gridded observations. For the purpose of this study, the North American Regional Reanalysis (NARR) [7] historical dataset, whose values are derived from the reanalysis of a 32 km resolution global NWP run, was used to initialize the WRF model.

B. Precipitation Type Algorithm

Although the WRF model allows users to select several physics options to help determine precipitation type, freezing rain (ZR) is not included as an output parameter. As the most prevalent form of ice accretion is from freezing rain, an effective method of forecasting precipitation type is required.

The process that results in freezing rain occurs when a hydrometeor falls to earth and exchanges heat with the air around it. A frozen hydrometeor falling in a warm layer ($> 0^{\circ}\text{C}$) will become liquid if the residence time (time to fall through the layer) is great enough. Similarly, a liquid hydrometeor falling through a cold layer ($< 0^{\circ}\text{C}$) will freeze completely if the residence time is great enough. Typically, a hydrometeor will become super cooled, i.e. remain in a liquid state, despite the fact that it is below 0°C . If a super cooled (or close to 0°C) hydrometeor comes into contact with an object that is also below freezing, the hydrometeor nucleates and immediately part of it turns to ice. As a result of this process, “freezing rain” requires a cold surface layer with a sufficiently deep warm layer above it.

For WILM, the precipitation type forecasting system was modeled after Ramer’s [8] precipitation type algorithm. Ramer diagnoses snow, freezing rain, ice pellets, rain, or mixed precipitation, using pressure, temperature, relative humidity, and wet bulb temperature. This selection was made partly based on the fact that the WRF model contains an output variable representing the “fraction of frozen precipitation,” denoted as SR, in the output variable set. To determine precipitation type, the value of SR is used to calculate an engagement factor, Γ , which acts as a multiplicative adjustment factor for the predicted model ice load.

After a series of hindcasts for a select number of locations for times during which freezing rain was observed and recorded, an optimized set of parameters for the engagement factor were selected. The selection was based on empirically choosing the parameters that minimize the ice load error.

WILM diagnoses freezing rain as follows. If SR falls in the range 0.00 – 0.01, liquid precipitation is assumed. If the temperature is also below 1.0°C , freezing rain is forecast ($\Gamma = 1$) and the ice accretion model is fully engaged. In this case, the “total grid scale precipitation” is considered to be freezing rain. If SR falls in the range 0.01 – 0.85 and the temperature is below 1.0°C , mixed precipitation is diagnosed and the ice accretion model is partially engaged as determined by Γ , which is found by (1). If SR rises above 0.85, the model diagnoses ice pellets and the ice accretion model is not

engaged. If the temperature is above 1.0°C the ice accretion model is not engaged.

$$\Gamma = 1 - \frac{SR - SR_{\text{u}}}{SR_{\text{u}} - SR_{\text{l}}}, \quad (1)$$

where SR_{l} and SR_{u} are the fuzzy top and bottom ranges respectively, and SR is the WRF model fraction of frozen precipitation variable.

C. Ice Accretion Model

A knowledge that freezing rain is occurring is not enough to determine the amount of ice accreted on power conductors; models must also be used to simulate ice growth. For this purpose, WILM uses Jones's Simple Model (SM) [9]. It is a numerical ice accretion model that determines ice accretion load by calculating the radial equivalent ice thickness (R_{eq}) using the intensity of freezing rain and wind speed. Assuming that all the precipitation forms a uniformly thick ice layer when freezing to a conductor, R_{eq} (mm) can be calculated by:

$$R_{\text{eq}} = \sum_{j=1}^n \frac{1}{\rho_{\text{i}}\pi} \left[(P_j \rho_{\text{w}})^2 + (3.6 V_j W_j)^2 \right]^{1/2}, \quad (2)$$

where ρ_{i} is the density of the ice accretion assumed to be 0.9 (g cm⁻³), P_j is the precipitation rate (mm hr⁻¹) in the j th hour, ρ_{w} is the density of water (1.0 g cm⁻³), V_j is the wind speed (m s⁻¹) in the j th hour, W_j is the liquid water content (g m⁻³) of the rain filled air in the j th hour ($W_j = 0.067 P_j^{0.846}$), and n is the duration of the storm in hours.

The term $P_j \rho_{\text{w}}$ represents the vertical flux of the falling rain, and $3.6 V_j W_j$ represents the horizontal flux of the rain due to wind. In the denominator, $\rho_{\text{w}}\pi$ accounts for both the expansion of water as it freezes, and the distribution of the water as it hits the ice covered cylinder and is (by assumption) uniformly spread over its surface. Jones et. al. [10] have used SM with observed meteorological conditions as model inputs, but SM can also use NWP variables as inputs.

After the radial equivalent ice thickness is known, the ice mass load can be obtained by first finding the mass load which corresponds to the the volume of ice multiplied by its density, as shown below.

$$m = \rho_{\text{i}} \cdot \pi \left(d \cdot R_{\text{eq}} + R_{\text{eq}}^2 \right) \cdot \ell, \quad (3)$$

where m is the ice mass (g), ρ_{i} is the ice density (0.0009 g mm⁻³), R_{eq} is the uniform radial ice thickness (mm), d is the conductor diameter (mm), and ℓ (mm) is the length of the conductor.

The weight load is found by multiplying the computed ice mass and the gravitational force and setting ℓ to one meter:

$$f_{\text{ice}} = 9.82 \cdot 10^{-3} \cdot \rho_{\text{i}} \cdot \pi \left(d \cdot R_{\text{eq}} + R_{\text{eq}}^2 \right), \quad (4)$$

where f_{ice} is the weight per unit length (N m⁻¹) of the accreted ice.

D. Wind Force Calculations

The final stage of the WILM system requires the calculation of the force exerted on the conductors due to wind and ice. Because these forces are prevalent in above ground conductors, transmission systems are built to withstand the loading caused by ice, wind, and wind with concurrent ice [11], [12]. The wind force model first calculates the force due to the weight of the ice, and the force of wind acting on the ice covered conductor, then calculates the vector sum of the results to determine the total force on the transmission conductor.

The wind force acting on an ice coated conductor is calculated following national standards. Equation (5) is the general formula for calculating wind force [13], and it can be extended with (6) and (7) [14].

$$\text{Load(N)} = 0.613 \cdot V^2 \cdot k_{\text{z}} \cdot G_{\text{RF}} \cdot I \cdot C_{\text{f}} \cdot A \quad (5)$$

$$q_o = \frac{1}{2} \lambda \mu \quad (6)$$

$$V = V_{\text{RX}} = K_{\text{R}} \cdot V_{\text{RB}} \quad (7)$$

In (5), 0.613 is the velocity-pressure coefficient that reflects the mass density of air at 15°C and an atmospheric pressure of 101.325 kPa. The coefficient of 0.613 should be used except where sufficient climatic data are available to justify the selection of a different value. The velocity-pressure coefficient 0.613 can be substituted by q_o as defined in (6); λ is the air density correction factor, normally equal to 1.0 (λ is defined in a table in [13] for other circumstances); μ is the air mass density. V is the wind speed (m s⁻¹) at 10 m above ground; V can be adjusted through equation (7) depending on the terrain category where the structure is located. In equation (7), V_{RB} is the reference wind speed; K_{R} is the adjustment factor found in Table 4 of [14]; k_{z} is the velocity-pressure exposure coefficient (line height dependent) found in Table 250-2 of [11]; G_{RF} is the gust response factor (line length and line height dependent) found in Table 250-3 of [14]; I is the importance factor, set to 1.0 for utility structures and their supported facilities; C_{f} is the force coefficient or the shape factor, equal to 1.0 for cylindrical structures and components; and A is the projected cross-sectional surface area of the ice coated conductor (m²). The extended wind force formulation is written as:

$$f_{\text{wind}} = 0.5 \cdot \lambda \cdot \mu \cdot (K_{\text{R}} \cdot V_{\text{RB}})^2 \cdot K_{\text{z}} \cdot G_{\text{RF}} \cdot I \cdot C_{\text{f}} \cdot \frac{d + 2R_{\text{eq}}}{1000}, \quad (8)$$

Thus, (4) is used to determine the load force due to the weight of accreted ice (f_{ice}) and (8) is used to determine the load force produced by wind blowing across the ice covered conductor (f_{wind}). Since both equations measure force in N m⁻¹, the vector sum of the two equations represents the total force exerted on a transmission conductor by both wind and ice.

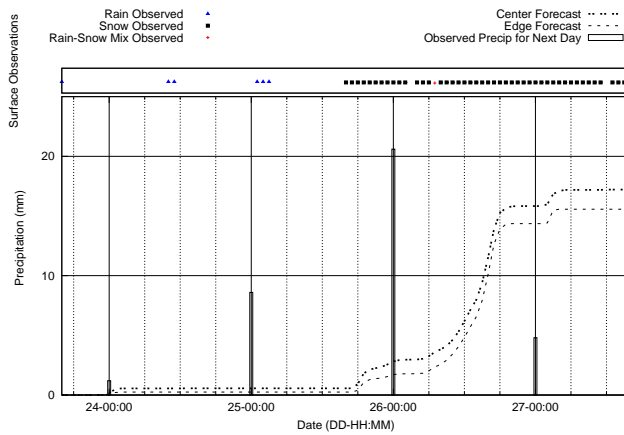


Fig. 1. Precipitation amount for Domain 3 over Vancouver International Airport (YVR) during November 24–26, 2008 (local time).

IV. NWP CALIBRATION

As previously described, WILM requires that the NWP model be reliable and accurate. To ensure this criterion is met, several hindcasts were performed for Vancouver International Airport (YVR) using the WRF model and then examined in order to test domain dynamics and physics options. The resulting data was compared against station data collected from both the CISL Research Data Archive (DS472.0) and Environment Canada’s website. The forecasts were compared in two ways: by computing error statistics for the numerical data (pressure, temperature, precipitation amount); and by using three of the most commonly used metrics: the probability of detection (POD), the false alarm rate (FAR), and the critical success index (CSI) on the model categorical data (i.e., was rain observed?).

To determine whether domain placement had an effect on the output of WRF simulations, two hindcasts were performed over YVR from November 24, 2006 (00:00 UTC) through November 28, 2006 (00:00 UTC). A “Center Run” domain placed YVR at the center grid point in the finest resolution domain (Domain 3), while the “Edge Run” setup placed YVR near the edge of Domain 3. Maps of surface pressures, temperature two meters above the surface, wind speed ten meters above the surface, and precipitation amounts from Domain 3 were visually examined. The maps showed similar features from both domain setups, even though both setups underpredicted precipitation amounts. However, the center run resulted in a closer match for precipitation with surface observations (see Figure 1); consequently, this was chosen as the best setup. The remainder of the simulations were performed with the location of interest centered in the finest resolution domain.

Finding an optimal configuration of the WRF model required repeated hindcasts of a location with known meteorological conditions. The effects of parameter changes in the hindcasts were studied by varying the settings for physics,

WRF Option	Value
mp_physics	6
mp_zero_out	0
ra_lw_physics	1
ra_sw_physics	1
sf_sfclay_physics	2
sf_surface_physics	1
bl_pbl_physics	2
cu_physics	3,3,0
diff_opt	1
km_opt	4
damp_opt	1
diff_6th_opt	0,0,0
mix_full_fields	.false.
time_steps	50 sec
input_from_file	.true.,.true.,.true.
radt	1 per dx
smooth_option	0
w_damping	1
grid_fdaa	1,0,0
g_fdaa_interval_m	180,180,180
fgdt	0,0,0
gfdaa_end_h	96,0,0

TABLE I
WRF PARAMETERS USED FOR WILM TESTS.

radiation, surface, and PBL schemes. Seventeen hindcasts were run for Vancouver International Airport and statistical scores were computed and examined. From these results, one particular WRF setup was determined to be the best, and whose configuration options are listed in Table I. Descriptions of these options can be found in [6].

V. WILM EVALUATION

To evaluate the WILM model, hindcasts were made for BC locations where known transmission failures occurred due to adverse weather. The results were analyzed to determine whether the modeled loads would exceed recommended specifications for the transmission unit in question; however, only one failure site included observations directly referencing radial equivalent ice thickness. This event occurred south of Squamish, British Columbia (-123.9° longitude, 49.6° latitude) on December 26, 2002. The location is on the border of “Medium Loading B” and “Heavy Loading” as per the Canadian Standard: Overhead Systems [14].

Assuming that the location lies in a Medium B category, the ice force, calculated by (4), can be applied with a conductor diameter of 30 mm and a radial equivalent ice thickness of 12.5 mm giving a design ice load of 14.7 N m^{-1} . To calculate the wind force, the ice covered cable diameter is considered. With a diameter of 30 mm (cable diameter) + (2 x 12.5 mm) (ice on both sides of cable), a cross-sectional width of 55 mm is found, giving an area of $0.055 \text{ m} \times 1 \text{ m} = 0.055 \text{ m}^2$. Using the Deterministic Weather Loads value from Overhead Systems Table 30 [14], the horizontal wind loading is 300 N m^{-2} , resulting in a wind loading of 16.5 N m^{-1} . Taking a vector sum of the ice force plus the wind on the ice force results in a total design loading of 22.10 N m^{-1} in this section of transmission line.

WILM determined the total ice and wind force loading using

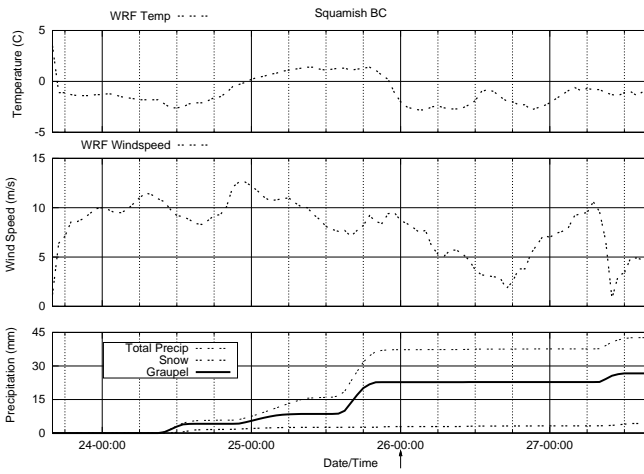


Fig. 2. Weather Data for the simulation of the transmission line failure south of Squamish, B.C. on December 26, 2002. The arrow (\uparrow) indicates the failure time. Time format is DD-HH:MM PST (local time).

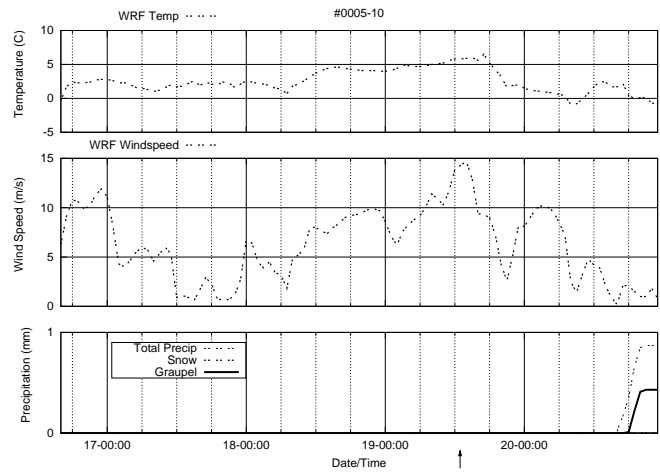


Fig. 4. Structure #0005-10 – Weather data for the simulation of the transmission line failure near Prince George on November 19, 2006. The arrow (\uparrow) indicates the failure time. Time format is DD-HH:MM PST (local time).

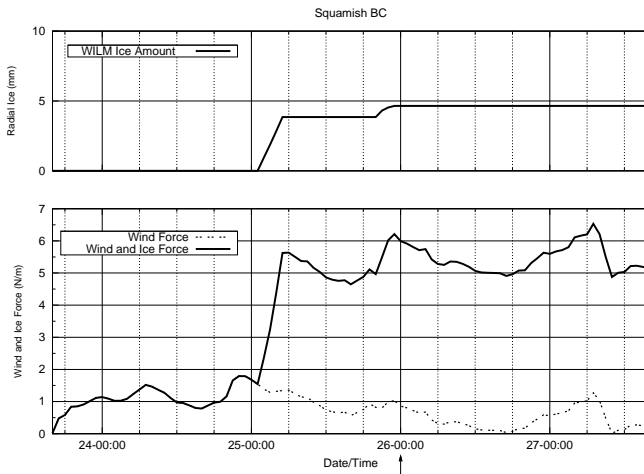


Fig. 3. Modeled data for the simulation of the transmission line failure south of Squamish, B.C. on December 26, 2002. The arrow (\uparrow) indicates the failure time. Time format is DD-HH:MM PST (local time).

(4) and (8). Here $\lambda = 1$, T = the simulated temperature two meters above ground level, and $K_R = 1.0$. It should be noted that even though the area is located in terrain corresponding to Category C, $K_R = 1.0$ was used, as the simulated wind speed already takes this into consideration. Additional, variable V_{RB} = the simulated wind speed in m s^{-1} at ten meters above the surface, $K_z = 1.0$, $G_{RF} = 0.91$, $I = 1.0$, $C_f = 1.0$, and cable diameter $d = 30$ mm.

The WILM simulated equivalent radial ice thickness was 4.65 mm and 2 mm of ice was observed on site. However, as shown in Figures 2 and 3, a maximum simulated combined wind and ice loading of only 6.21 N m^{-1} was present just prior to the fault.

Several other failure sites with reported damage related to weather phenomena were simulated, and wind and ice load

values were calculated. Failures due to high wind occurring near Prince George, B.C. on November 19, 2006 at 12:54 were simulated and produced the following results:

- Structure #0005-10 failed with a wind and ice load of 2.47 N m^{-1} , results listed in Figures 4 and 5.
- Structure #0010-SUB failed with a wind and ice load of 2.49 N m^{-1} , results listed in Figures 6 and 7.
- Structure #0000-00S failed with a wind and ice load of 1.37 N m^{-1} , results listed in Figures 8 and 9.

Another failure occurred to the north-east of Stewart, B.C. on November 12, 1990 (no time given). This event was responsible for 12 outages due to snow loading and heavy ice. The model produced a maximum simulated wind and ice force of 2.45 N m^{-1} , shown in Figures 10 and 11.

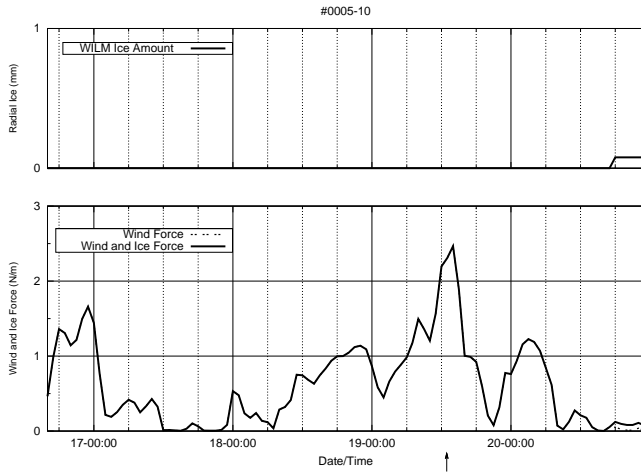


Fig. 5. Structure #0005-10 – Modeled data for the simulation of the transmission line failure near Prince George on November 19, 2006. The arrow (↑) indicates the failure time. Time format is DD-HH:MM PST (local time).

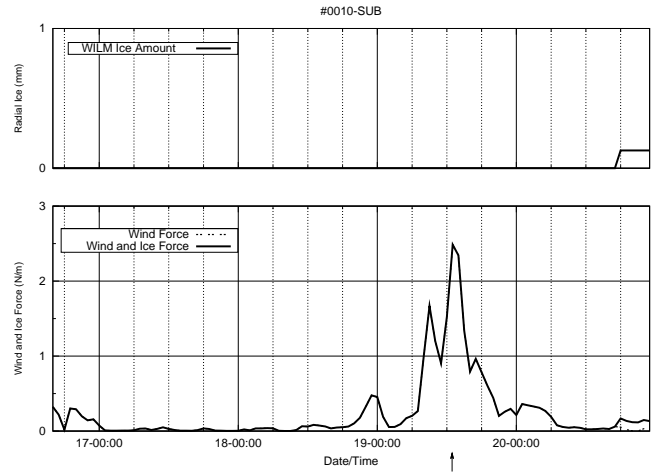


Fig. 7. Structure #0010-SUB – Modeled data for the simulation of the transmission line failure near Prince George on November 19, 2006. The arrow (↑) indicates the failure time. Time format is DD-HH:MM PST (local time).

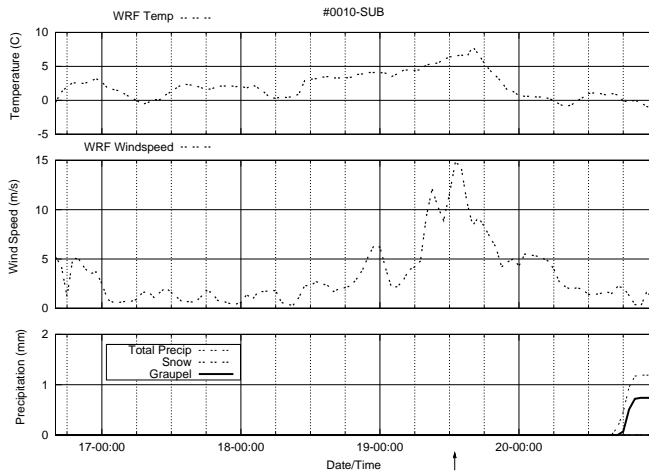


Fig. 6. Structure #0010-SUB – Weather data for the simulation of the transmission line failure near Prince George on November 19, 2006. The arrow (↑) indicates the failure time. Time format is DD-HH:MM PST (local time).

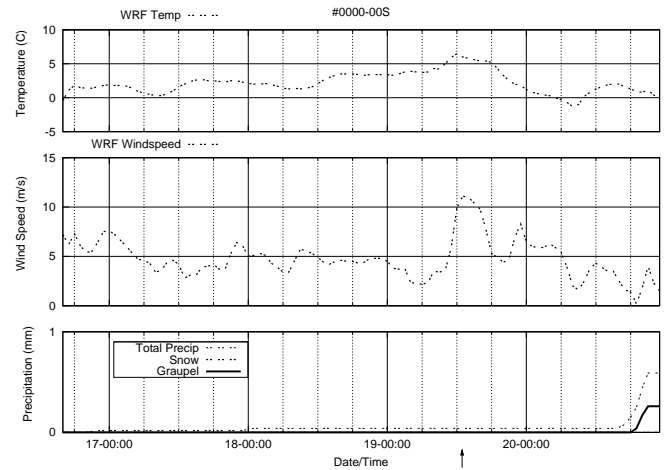


Fig. 8. Structure #0000-00S – Weather data for the simulation of the transmission line failure near Prince George on November 19, 2006. The arrow (↑) indicates the failure time. Time format is DD-HH:MM PST (local time).

VI. DISCUSSION

The output of WILM produced similar wind and ice force values near times of failure ($\approx 3 \text{ N m}^{-1}$); however, they are an order of magnitude smaller than the design loadings ($\approx 22 \text{ N m}^{-1}$). There are several possible explanations for the discrepancies:

- NWP systems are prone to error in forecasting wind gusts. Thus, wind gusts near failure times may have caused an excess load on the conductors.
- Forces not accounted for by WILM could have been present. The wind and ice force on the support structures was not examined; it could dramatically increase the total force applied to the system
- WILM considers only ice accretion due to freezing rain.

If in-cloud icing occurred, it could have increased the total load at the failure sites.

- The force due to conductor galloping was also not considered by WILM. Safety codes describe the effects of conductor galloping [11]; however they do not specify a method for determining the produced forces. Some authors state that only a small amount of ice is needed for the process to occur [15] and fluctuations in wind speed over time periods as short as 30 seconds can start galloping [16]. Although many authors have studied the effects of galloping [17], [18], [19], [20], it is still not well understood and so it has not been included in the WILM system.
- Information about the state of the transmission network

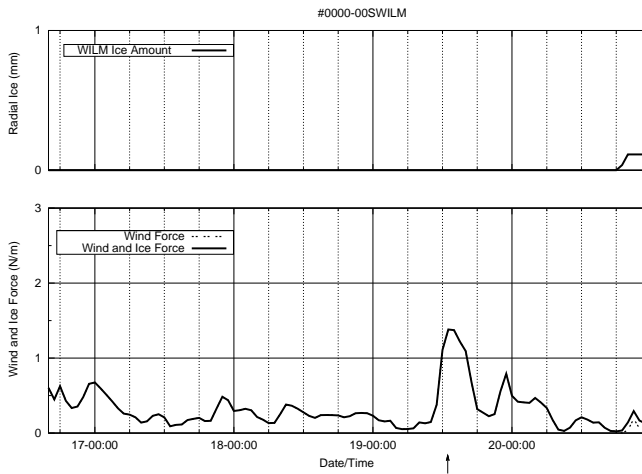


Fig. 9. Structure #0000-00S – Modeled data for the simulation of the transmission line failure near Prince George on November 19, 2006. The arrow (↑) indicates the failure time. Time format is DD-HH:MM PST (local time).

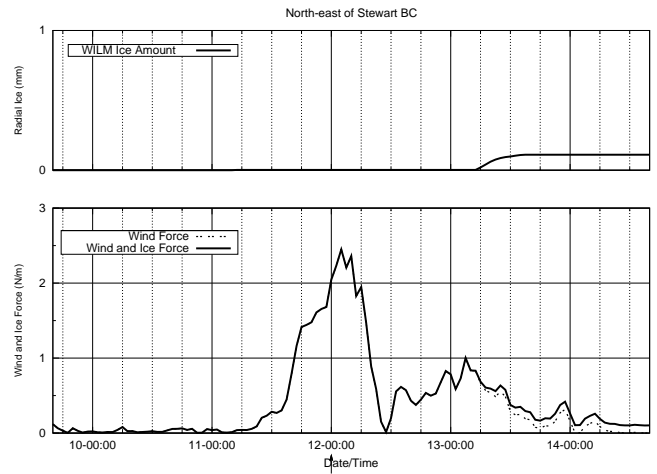


Fig. 11. Modeled data for the simulation of the transmission line failure north-east of Stewart, B.C. on November 12, 1990. The arrow (↑) indicates the failure time. Time format is DD-HH:MM PST (local time).

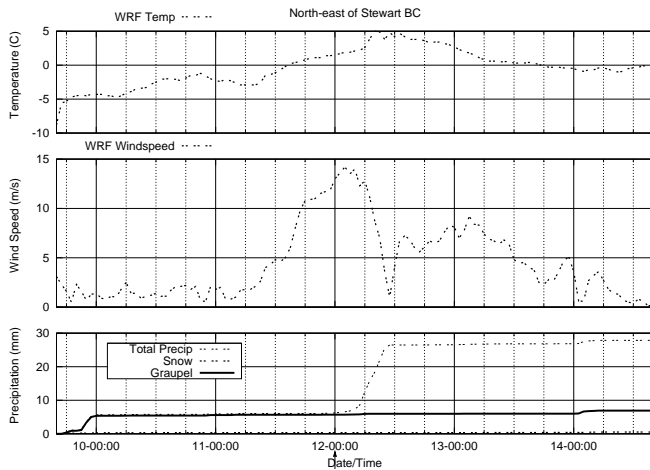


Fig. 10. Weather data for the simulation of the transmission line failure north-east of Stewart, B.C. on November 12, 1990. The arrow (↑) indicates the failure time. Time format is DD-HH:MM PST (local time).

prior to the failure events was not known. Perhaps the sections of the network that experienced faults contained components that were fatigued or damaged by previous storms; therefore, they would be more likely to fail under lower force loadings than the original loadings for which they were designed to support.

VII. SUMMARY AND FUTURE WORK

In this paper, WILM was used to hindcast meteorological conditions relevant to power transmission failures, specifically, the wind and ice loads caused by ice accretion from freezing rain. The core of WILM is composed of the WRF numerical weather prediction system, coupled with a precipitation type determination algorithm based on the Ramer algorithm, Jones’s Simple Model ice accretion algorithm and a wind on

ice force load model.

To optimize the WRF NWP system used by WILM, a series of trials were conducted for Vancouver International Airport for November 2006 during which a wind storm was observed. Surface data was compared and subsequently used to select the optimal WRF configuration. This configuration was then used by WRF to simulate meteorological conditions over areas of the BC interior where BCTC had documented weather related power transmission failures. WILM’s wind loading component was used to retroactively predict maximum loading values just prior to the documented failure times and compared with expected loading conditions.

There are still several areas in which WILM can be improved. Firstly, the main limitation of the presented system is the presence of cascading errors. WILM is susceptible to compounded errors, as errors in forecasted meteorological variables move through the WILM components. The NARR data used to initialize the model was derived from a reanalysis of a 32 km resolution global NWP model that has been corrected for obvious errors, but residual observation and model errors remain. The WRF system will amplify errors in the initial conditions and introduce new errors as the result of deficiencies in the model physics, dynamics, radiation schemes, etc.

Secondly, the WRF system is a new and very complex model with many configurable options that are constantly being updated. Although the system presented in this paper was tested using various physics and dynamics packages, optimization was performed for only one time and location. It may be possible that WRF options that work well for one type of landscape do not necessarily work well in other regions. Also, the vertical levels used in the simulation can be varied by both height and number. Described tests were performed using the default number and heights of the vertical levels; however, this is not guaranteed to be an optimal setup. Thus, successful

use of WILM to predict loads and forces over large areas requires further evaluation and testing of the various WRF configuration options.

Thirdly, extending the capabilities of WILM to include the forecasting of ice accretion also requires more study. WRF was run with initial conditions from NARR, a historical data set. Reanalysis implies that obvious errors have been corrected and the original analyses have been updated. To evaluate a forecasting implementation of the WILM, the use of real-time input conditions, such as the National Center for Environmental Prediction (NCEP) global ensemble forecast system, the North American Mesoscale Model, or the NCEP FNL Global Analysis, needs to be tested.

Fourthly, the selection of fuzzy values to determine the engagement factor of the SM was done subjectively. A more objective study using computational intelligence optimization techniques to discover a better combinations of parameters is expected to remove human bias [21] and thus improve the overall accuracy of the ice and force load forecasts.

Finally, more simulations need to be conducted over areas where power transmission failures have been observed. A full investigation will require more case studies and detailed specifications of the failure sites including: times, locations, direction of conductors, number of conductors on poles, height of conductors, and composition of structures (wood, steel, single pole, lattice structure, etc). This information could result in more meaningful comparisons between model outputs and observations.

ACKNOWLEDGMENT

This work was supported by the Natural Sciences and Engineering Research Council of Canada (NSERC), Mathematics of Information Technology and Complex Systems (MITACS) and British Columbia Transmission Corporation (BCTC).

REFERENCES

- [1] C. Crocombette, "The weather impact on the transmission of electricity in France," in *8th European Conference on Applications of Meteorology ECAM'07*, El Escorial, Spain, October 2007.
- [2] K. Eben, P. Juras, J. Keder, I. Vyorkova, and E. Pelikan, "Using MM5 to predict hazardous situations for power supply," in *PSU/NCAR Mesoscale Model Users' Workshop*, vol. 13, 2003, pp. 52 – 55.
- [3] F. Kiessling, P. Nefzger, J. Nolasco, and U. Kaintzyk, *Overhead Power Lines: Planning, Design, Construction*. Springer-Verlag, 2003, no. ISBN: 3540002970.
- [4] C. Sullivan, V. Petrenko, J. McCurdy, and V. Kozliouk, "Breaking the ice," *IEEE Industry Applications Magazine*, pp. 49–54, October 2003.
- [5] E. Lecomte, A. Pang, and J. Russell, *Ice Storm '98*, ICLR Research Paper Series - No. 1, 1998.
- [6] W. C. Skamarock, J. B. Klemp, J. Dudhia, D. O. Gill, D. M. Barker, W. Wang, and J. G. Powers, "A description of the advanced research WRF version 2," Tech. Rep., 2005.
- [7] N. C. for Environmental Prediction, "North american regional reanalysis homepage," Online at www.emc.ncep.noaa.gov/mmb/rrean/, July 2007, (Accessed on Jan. 4, 2009).
- [8] J. Ramer, "An empirical technique for diagnosing precipitation type from model output." in *Preprints, Fifth International Conference on Aviation Weather Systems, American Meteorological Society*, Vienna, VA, August 2-6 1993, pp. 227–230.
- [9] K. Jones, "A simple model for freezing rain ice loads," *Atmospheric Research*, vol. 46, pp. 87–97, 1998.

- [10] K. Jones, A. Ramsay, and J. Lott, "Icing severity in the December 2002 freezing-rain storm from ASOS data," *Monthly Weather Review*, vol. 132, pp. 1630–1644, 2004.
- [11] *National electrical safety code - C2-2007*, 2007th ed., The Institute of Electrical and Electronics Engineers, Inc., 3 Park Avenue, New York, NY, August 2006.
- [12] D. Marne, *National Electrical Safety Code*, S. Chapman, Ed. McGraw-Hill Companies, Inc., 2007.
- [13] "Design criteria of overhead transmission lines - Third edition: CEI/IEC 60826:2003," Canadian Standards Association, Tech. Rep. C22.3 No. 60826-06-CAN/CSA, October 2006.
- [14] "Overhead systems - Eighth edition," Canadian Standards Association, Tech. Rep. C22.3 No. 1-06, October 2006.
- [15] P. McComber and A. Paradis, "A cable galloping model for thin ice accretions," *Atmospheric Research*, vol. 46, pp. 13–25, 1998.
- [16] T. Ohkuma, J. Kagami, H. Nakauchi, T. Kikuchi, K. Takeda, and H. Marukawa, "Numerical analysis of overhead transmission line galloping considering wind turbulence," *Electrical Engineering in Japan*, vol. 131, pp. 1386 – 1397, 2000, translated from Denki Gakkai Ronbunshi, Vol. 118-B, No. 12, December 1998, pp. 1386-1397.
- [17] M. A. Baenziger, W. D. James, B. Wouters, and L. Li, "Dynamic loads on transmission line structures due to galloping conductors," *IEEE Transactions on Power Delivery*, vol. 9, no. 1, pp. 40–49, January 1994.
- [18] O. Chabart and J. L. Lilien, "Galloping of electrical lines in wind tunnel facilities," *Journal of Wind Engineering and Industrial Aerodynamics*, vol. 74-76, pp. 967–976, 1998.
- [19] Y. M. Desai, P. Yu, N. Popplewell, and A. H. Shah, "Finite element modelling of transmission line galloping," *Computers & Structures*, vol. 57, no. 3, pp. 407–420, 1995.
- [20] C. B. Gurung, H. Yamaguchi, and T. Yukino, "Identification of large amplitude wind-induced vibration of ice-accreted transmission lines based on field observed data," *Engineering Structures*, vol. 24, pp. 179–188, 2002.
- [21] A. H. Wright, "Genetic algorithms for real parameter optimization," in *Foundations of Genetic Algorithms*. Morgan Kaufmann, 1991, pp. 205–218.